

Resist double patterning on BARCs and spin-on multilayer materials

Douglas J. Guerrero, Daniel M. Sullivan, Ramil-Marcelo L. Mercado
Brewer Science Inc., 2401 Brewer Drive, Rolla, Missouri 65401 USA

ABSTRACT

Many approaches to double patterning have been devised, of which most have been designed to reduce the number of process steps. The litho-freeze-litho-etch process (LFLE) is one such technique that eliminates the first etch step from the standard litho-etch litho-etch (LELE) process. The resist freeze material chemically modifies the patterned photoresist, as well as potentially the layer beneath, which may result in a performance change at the second lithography step. Another approach, litho-process-litho-etch (LPLE) does not involve the use of a chemical freeze material, instead relying on a thermal treatment to remove excess solvent from the polymer and differential energy of activation between two resists to create a double-patterned image. Finally, double patterning using negative-tone development of a positive-acting photoresist is another approach in consideration. In this paper, we present the results of several double-patterning processes on organic bottom anti-reflective coatings (BARCs) and spin-on multilayer stacks consisting of a silicon hardmask on top of a carbon underlayer. Pattern profiles of the first and second lithography steps are compared.

Keywords: double patterning, multilayer, anti-reflective, spin-on, LFLE, LPLE, negative-tone development

1. INTRODUCTION

Currently, double patterning is preferred to generate complex (i.e., non-repeating) features smaller than 40 nm using water immersion-based optical lithography toolsets.¹ LELE is the most mature process to enable double patterning, but it is also the most cost-prohibitive. Alternative processes are being developed to eliminate one etch process and reduce cost. Of these, LFLE^{2,3} and LPLE^{4,5} have been shown to form line-space (L/S) patterns of 32-nm half-pitch and smaller.

Another process that has been developed with applicability for double patterning is negative-tone development of a positive-working photoresist system.^{6,7} This concept is targeted toward trench and contact hole printing where it is more difficult to get a good aerial image with the use of a dark field mask. This method overcomes that limitation by using exposures with a bright field mask and developing out the unexposed areas using an organic solvent instead of a tetramethylammonium hydroxide (TMAH) developer.

This paper describes the use of the double-patterning processes described above to print 32-nm features on organic BARCs and 45-nm half-pitch features on a multilayer stack. Similar methodologies and necessary modifications are applied to obtain similar results from a spin-on stack consisting of the carbon-rich layer, silicon hardmask, and photoresist. The goal of this study is to demonstrate the applicability of one or more double-patterning techniques and processes to a spin-on stack (Figure 1), as such a stack with four spin-on layers further reduces the cost of device fabrication by keeping the materials within the lithography cluster as much as possible. (The polysilicon and oxide layers are not part of the total spin-on system.) While the processes are intended to include etch behavior (i.e., LFLE and LPLE), only lithographic considerations are included as part of this study.

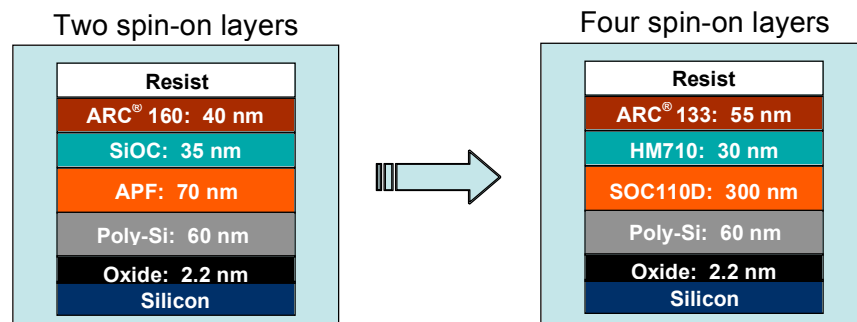


Figure 1. Proposed spin-on alternatives to current integrated circuit fabrication stack components.

2. EXPERIMENTAL

2.1 Materials

The BARC materials used in this study were ARC[®] 29SR, ARC[®] 86, ARC[®] 133, and ARC[®] 160 coatings (Brewer Science). The multilayer stack consisted of OptiStack[®] HM710 material as the silicon-containing hardmask and OptiStack[®] SOC110 material as the carbon underlayer (Brewer Science).

Photoresists used were Pi6-001 and PP007Tr2 (Tokyo Ohka Kogyo [TOK]) for LPLE. Resists 1 and 2 from JSR were used to evaluate the LFLE process as well as a proprietary chemical freeze agent. The NTD process used FAIRS-A19A as the photoresist, FN-DP001 as the developer, and RP002 for the rinse (FujiFilm Electronic Materials).

2.2 Simulations

Modeling was performed using PROLITH software, v.11.

2.3 Lithographic Conditions

Films were coated and baked on a Sokudo[®] R3 track system. Lithography was performed on an ASML[™] XT1900i scanner. Optical settings varied and are reported in each set of data.

Imaging for the LFLE process used the following scanner conditions: numerical aperture (NA) = 1.0, illumination = quadrupole (DOE dipole40X), y-polarized, $\sigma = 0.85/0.65$, and MCD40.

Imaging for the LPLE process used the following scanner conditions: NA = 1.0, illumination = quadrupole (DOE dipole40X), y-polarized, $\sigma = 0.85/0.65$, and MCD56.

Imaging for the negative-tone development process used the following scanner conditions: NA = 1.2, illumination = dipole40X, y-polarized, and $\sigma = 0.987/0.844$.

2.4 Metrology

Critical dimension (CD) SEM measurements were carried out in Hitachi S-9280 and KLA eCD1 CD SEM systems.

3. RESULTS AND DISCUSSION

3.1 L/S Patterning on BARC

3.1.1. LFLE Process

Three different BARCs, ARC[®] 86, ARC[®] 133, and ARC[®] 160 coatings, were evaluated for their compatibility with the two different photoresists, the freeze chemical, and the associated processing conditions. Resist compatibility was checked for performance for the individual resists that are used in the process.

Resist 1 was patterned at 32-nm (1:3 L/S) on 55 nm of the three various BARCs. Results are shown in Figure 2.

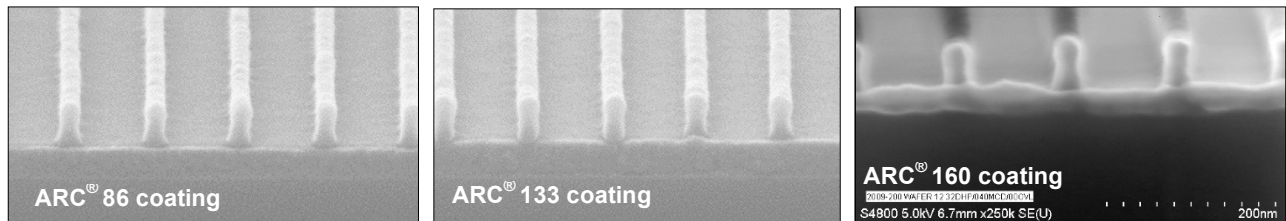


Figure 2. Profiles obtained of LFLE Resist 1 on various BARCs.

A slight footing profile was obtained on both ARC[®] 86 and ARC[®] 160 coatings, which have similar polymer chemistries. ARC[®] 133 coating showed the straightest profile, which may be due to better compatibility of its acrylate polymer system with that used in the photoresist.

After the first lithography step, the patterned wafers were then subjected to the chemical freeze treatment to render the photoresist pattern insoluble to the application of the second photoresist. In the ideal case, no changes are expected to occur. The cross-section profiles were checked for any changes relative to the prior step (Figure 3).

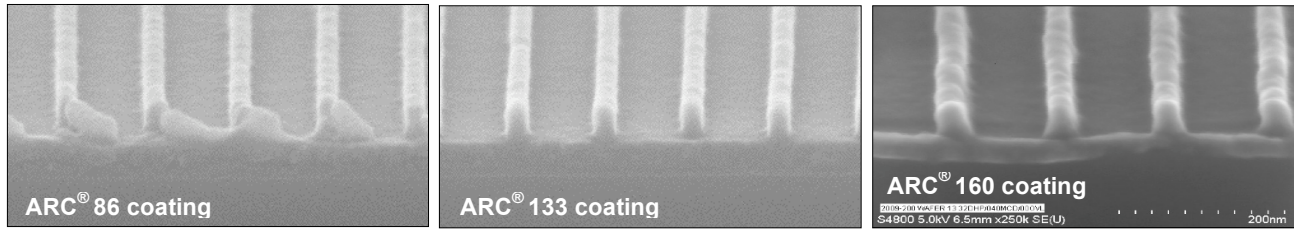


Figure 3. Profiles of Resist 1 on various BARCs after the chemical freeze process.

In all three cases, after the freeze step, the resist profiles showed a slight foot. Footing had worsened in the case of ARC[®] 86 and ARC[®] 160 coatings. Also noticeable is the top loss in each case.

Dense 32-nm HP patterns were then generated by applying and imaging Resist 2 with the same pitch 32-nm (1:3 L/S) as the first pattern density in Resist 1. Results are shown in Figure 4.

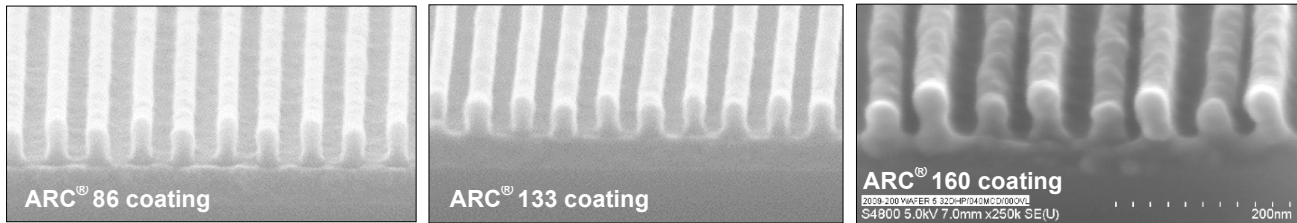


Figure 4. Dense 32-nm L/S features from LFLE double patterning on various BARCs.

From the profiles shown, ARC[®] 160 coating shows a high level of footing, and pronounced resist height differences between patterning steps 1 and 2. ARC[®] 86 and 133 coatings also show some footing and resist height differences, but these are not as severe. Comparing the latter two BARCs, profiles obtained for ARC[®] 133 coating are straighter and qualitatively show lower line roughness compared to ARC[®] 86 coating profiles.

3.1.2 LPLE

ARC[®] 29SR coating was used for the LPLE evaluation. As was the case in LFLE patterning, a first round of lithographic evaluation (32-nm [1:3 L/S]) was performed using Pi6-001 resist on ARC[®] 29SR coating. Results are shown in Figure 5. The profiles obtained show a slight footing behavior, similar to that seen for ARC[®] 86 coating and Resist 1 in the LFLE case. From cross-section analysis, an exposure latitude of about 17% was obtained from the first pass (Figure 6).

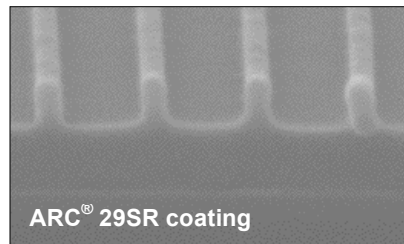


Figure 5. 32-nm L/128-nm P patterns of Pi6-001 resist on ARC[®] 29SR at best dose and focus.

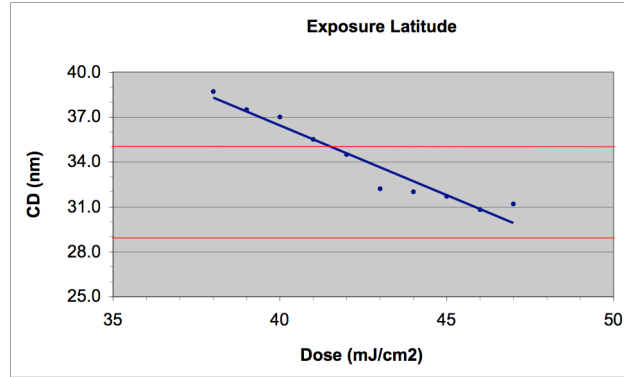


Figure 6. Exposure latitude data for litho 1 (L1) step of Pi6-001 resist on ARC[®] 29SR coating.

In the next step of evaluations, two different resists, Pi6-001 and PP007Tr2, were imaged as 32-nm (1:3 L/S) patterns and overlaid to form dense 32-nm features. The results are shown in Figure 7.

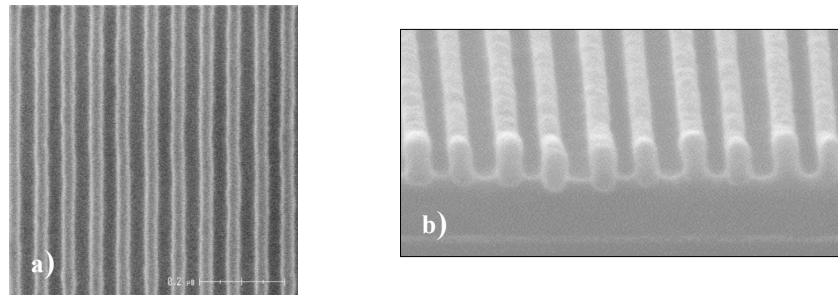


Figure 7. a) Top-down image of 32-nm L/S patterns obtained by the LPLE process (L1: 32 mJ/cm²; L2: 37 mJ/cm²) and b) cross-section image of 32-nm L/S patterns obtained by the LPLE process at best dose and focus.

The profiles are fairly straight, with little differences between the first and second patterns. The top loss is also less pronounced compared to the LFLE process described earlier.

3.2 L/S Patterning on Multilayer Stack

3.2.1 LFLE

Similar to the evaluation performed for the BARC, the individual resists (Resists 1 and 2) were tested for lithographic compatibility with the stack composed of an HM710 layer (30 nm) on top of an SOC110D (300 nm) layer. Unfortunately, severe line collapse was observed when applying Resist 1 directly on top of the HM710 coating. The smallest critical dimension successfully obtained was 35 nm (Figure 8a). Correct 32-nm L/128-nm P features were obtained when ARC[®] 133 coating (55 nm) was applied on top of the HM710 layer (Figure 8b). Addition of the BARC also improved the exposure latitude, as well as the overall process window (Figure 9). Resist 2 was compatible with a direct application on the hardmask and was able to produce 32-nm L/128-nm P features (Figure 8c.). Resist 2 on the HM710 layer also had good exposure latitude, even without a BARC present.

The profiles are excellent, in all cases better than that obtained from the BARC comparison earlier. There is no discernible foot. However, the results for Resist 1 prevented us from demonstrating LFLE double patterning on a trilayer (resist-hardmask-carbon) stack. Since it was demonstrated earlier that Resist 2 is compatible with ARC[®] 133 coating, we plan on demonstrating the LFLE process on a quad-layer (resist-BARC-hardmask-carbon) stack in the future.

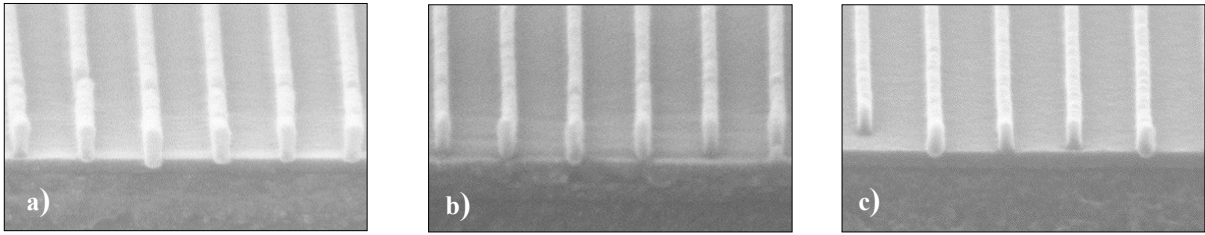


Figure 8. a) 35-nm line features using Resist 1 on HM710 hardmask and SOC110D spin-on carbon layer. b) 32-nm line features using Resist 1 on a stack composed of ARC[®] 133/HM710/SOC110D layers. c) 32-nm line features using Resist 2 on HM710 and SOC110D layers.

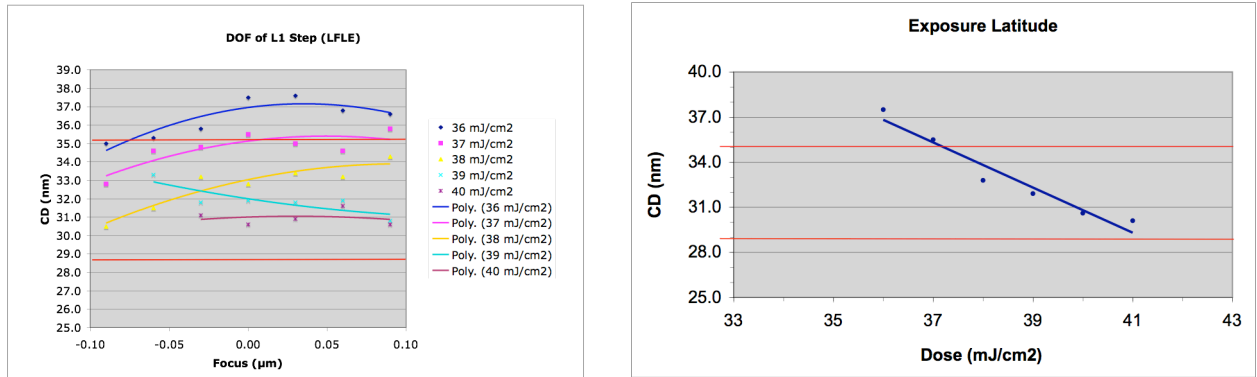


Figure 9. Process window of resist 1 (32-nm [1:3 L/S]) obtained by applying 55 nm of ARC[®] 133 coating on 30 nm of OptiStack[®] HM710 coating and 300 nm of SOC110D coating.

3.2.2 LPLE

Resist compatibility of Pi6-001 resist and PP007Tr2 resist were evaluated on the stack composed of the HM710 hardmask and SOC110D layer. Both resists were found to have good compatibility directly on the hardmask and show good process windows (Figure 10).

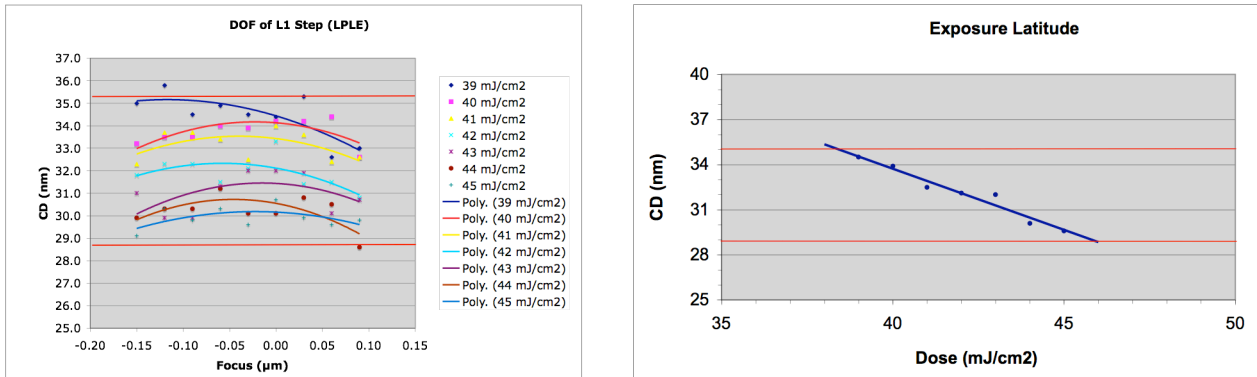


Figure 10. Process window data for 32-nm L/128-nm P Pi6-001 resist on the stack made from OptiStack[®] HM710 and SOC110D layers.

Profiles obtained using the individual resists with 32-nm L/128-nm P features are shown in Figure 11. Each case shows good profiles, better than the BARC case, and thus are promising candidates to continue with the LPLE process as a trilayer stack.

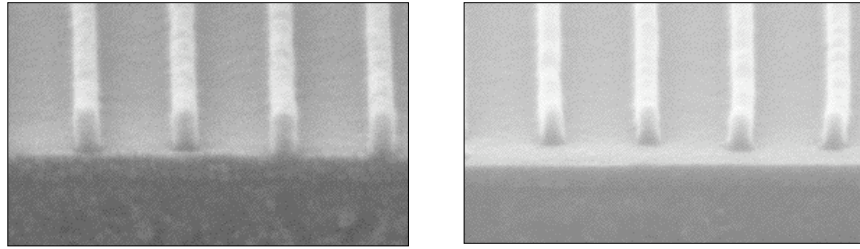


Figure 11. 32-nm (1:3 L/S) features using Pi6-001 (left) and PP007Tr2 (right) resists on stack made with HM710 (30 nm) and SOC110D (300 nm) layers.

3.3 Contact Hole Printing Using Negative-Tone Development

Negative-tone development is a different means to achieve double patterning. In this process, a positive-working resist is applied to the substrate and exposed two times, each at low doses, and the resist areas that are double-exposed become fully deprotected. An organic-based developer is then used to remove the unexposed areas, leaving a negative-tone image.

This method was evaluated as a means to generate dense contact hole features on a spin-on stack. However, poor adhesion, similar to that seen in the LFLE process, was observed. Again in this case, this was addressed by the application of ARC[®] 133 on top of the hardmask, making a quad-layer stack. The quad-layer stack using FAIRS-A19A photoresist was successfully imaged and developed to form a dense array of 45-nm contact holes (Figure 12). These were obtained while having a reasonable process latitude (Figure 13).

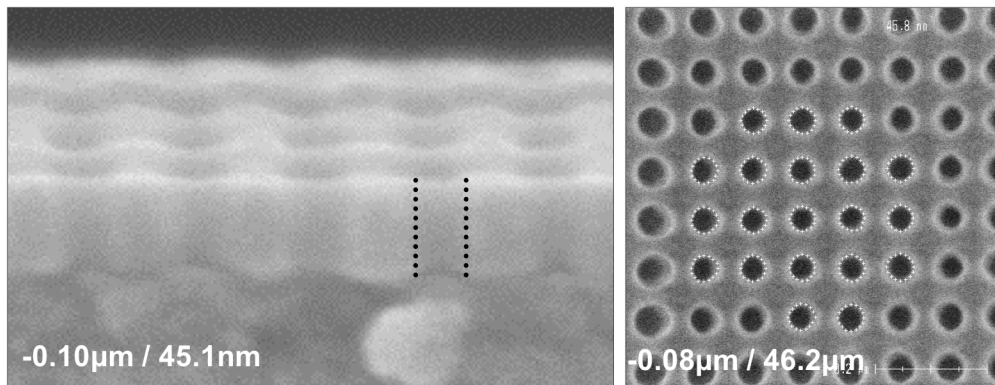


Figure 12. Array of dense 45-nm contact holes obtained by negative-tone development of FAIRS-A19A resist on ARC[®] 133 (55 nm)/HM710 (30 nm)/SOC110D (300 nm) stack layers.

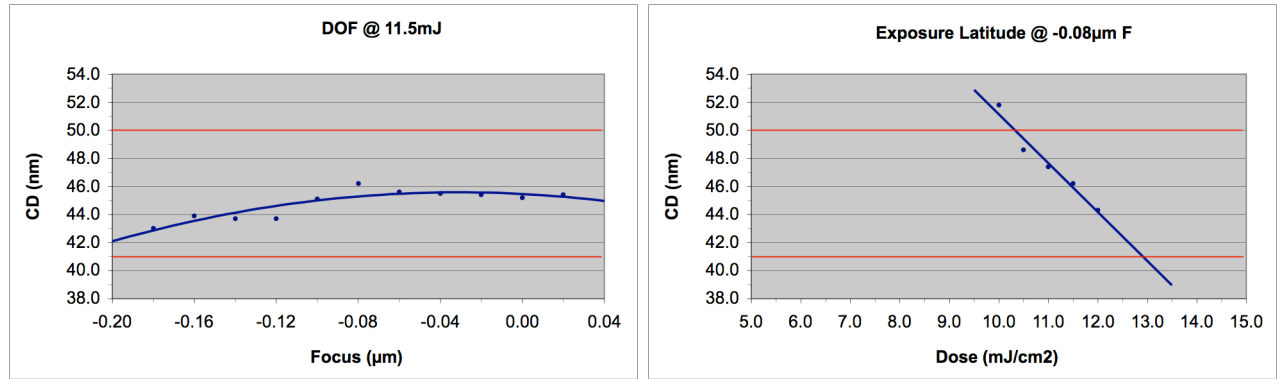


Figure 13. Process window information for dense 45-nm contact hole printing using negative-tone development.

In comparing the three methods by which double patterning on spin-on multilayer stacks may be achieved without having to go through two subsequent etch steps, it can be seen that, in some cases, the use of an organic BARC may be beneficial. This is seen in the LFLE and NTD processes. Assuming a thickness of 300 nm for the OptiStack[®] SOC110D layer, reflectivity curves were generated using 30 nm of HM710 hardmask alone on top of the spin-on carbon layer, as well as 55 nm of ARC[®] 133 coating on 30 nm of the HM710 hardmask (Figure 14). The BARC maintains reflection control of the hardmask while providing the additional improvements in overall process latitude, DOF, EL, adhesion, etc. The experimental results on BARC alone as well as on multilayer stacks show that the BARC acts as a compatibility enhancement layer, widening the available process window, or even providing a working window when none exists when BARC is not used.

SUMMARY AND CONCLUSIONS

Double patterning processes, LFLE, and LPLE were demonstrated on organic BARCs applied on silicon. Preliminary investigations showed that the use of a BARC on a spin-on hardmask and carbon layer improves the resist compatibility as well as widens the available process window.

Double patterning of dense 45-nm contact holes were demonstrated using the negative-tone development process on a quad-layer stack comprised of FAIRS A19A resist, ARC[®] 133 coating, OptiStack[®] HM710 hardmask, and SOC110D spin-on carbon layer.

In cases where BARC is used, its primary function was chemical in nature, providing resist compatibility and increased adhesion to the substrate, and was not so much for the purpose of reflection control.

ACKNOWLEDGMENTS

The authors would like to thank JSR Micro, TOK, and FujiFilm Electronic Materials for permission to use their photoresists and baseline processes for this study. We would also like to thank Runhui Huang and Yubao Wang for providing the BARC and multilayer materials used in this study.

REFERENCES

- [1] S. Shimura, M. Kushibiki, T. Kawasaki, R. Tanaka, A. Tokui, Y. Ishii, "Fine trench patterns with double patterning and trench shrink technology," *Proceedings of SPIE*, vol. 7273, 72730A (2009).

- [2] G. Wakamatsu, Y. Anno, M. Hori, T. Kakizawa, M. Mita, K. Hoshiko, T. Shioya, K. Fujiwara, S. Kusumoto, Y. Yamaguchi, T. Shimokawa, "Double patterning process with freezing technique," *Proceedings of SPIE*, vol. 7273, 72730B (2009).
- [3] T. Kakizawa, G. Wakamatsu, Y. Anno, M. Hori, M. Mita, K. Hoshiko, T. Shioya, K. Fujiwara, S. Kusumoto, Y. Yamaguchi, T. Shimokawa, "Freezing material development for double patterning process," *Journal of Photopolymer Science and Technology*, vol. 22, no. 5, pp. 641-646 (2009).
- [4] T. Nakamura, M. Takeshita, S. Maemori, R. Uchida, R. Takasu, K. Ohmori, "Newly developed positive tone resists for posi/posi double patterning process," *Proceedings of SPIE*, vol. 7273, 727304 (2009).
- [5] T. Nakamura, R. Takasu, P. Wong, M. Maendhout, "Process Feasibility Investigation of Freezing Free Process," *Journal of Photopolymer Science and Technology*, v. 22, no. 5, pp. 647-652 (2009).
- [6] S. Tarutani, T. Hideaki, S. Kamimura, "Development of materials and processes for negative tone development toward 32-nm node 193-nm immersion double-patterning process," *Proceedings of SPIE*, vol. 7273, 72730-C (2009).
- [7] S. Tarutani, H. Tsubaki, S. Kamimura, "Materials and processes of negative tone development for double patterning process," *Journal of Photopolymer Science and Technology*, v. 22, no. 5, pp. 635-640 (2009).